Correlations Between Dark-Adapted Rod Threshold Elevations and ERG Response Deficits in Duchenne Muscular Dystrophy

Mirella Telles Salgueiro Barboni,[1,2] Sarah Leonardo Dias,[2] Leonardo Aparecido Silva,[2] Francisco Max Damico,[2,3] Kallene Summer Vidal,[2] Marcelo Fernandes Costa,[2] Balázs Vince Nagy,[4] Jan Kremers,[5] and Dora Fix Ventura[2]

[1]Department of Ophthalmology, Semmelweis University, Budapest, Hungary
[2]Department of Experimental Psychology, Institute of Psychology, University of Sao Paulo, Brazil
[3]Department of Ophthalmology, Faculty of Medicine, University of Sao Paulo, Brazil
[4]Department of Mechatronics, Optics and Mechanical Engineering Informatics, Budapest University of Technology and Economics, Budapest, Hungary
[5]Section for Retinal Physiology, University Hospital Erlangen, Erlangen, Germany

Correspondence: Mirella Telles Salgueiro Barboni, Department of Ophthalmology, Semmelweis University, 1085 Budapest, Mária u. 39., Hungary; mtsbarboni@gmail.com.
Dora Fix Ventura, Department of Experimental Psychology, University of Sao Paulo, Prof. Mello de Morais, 1721, 05508-030 Sao Paulo, Brazil; dventura@usp.br.

MTSB and SLD contributed equally to the paper.

Received: October 19, 2020
Accepted: April 3, 2021
Published: April 23, 2021

Citation: Barboni MTS, Dias SL, Silva LA, et al. Correlations between dark-adapted rod threshold elevations and ERG response deficits in Duchenne muscular dystrophy. *Invest Ophthalmol Vis Sci.* 2021;62(4):29. https://doi.org/10.1167/iovs.62.4.29

Purpose. The purpose of this study was to characterize changes in the full-field flash electroretinogram (ERG) in association with psychophysical dark-adapted visual thresholds in patients with genetically characterized Duchenne muscular dystrophy (DMD) either lacking Dp427 (Up 30) or at least Dp260 in addition to Dp427 (Down 30).

Methods. Twenty-one patients with DMD and 27 age-similar controls participated in this study. Dark-adapted (0.01, 3.0, and 10 cd.s/m^2 flashes) and light-adapted (3.0 cd.s/m^2 flash) ERGs were recorded following International Society for Clinical Electrophysiology of Vision (ISCEV) standard protocols. Visual detection thresholds to 625-nm (cone function) and 527-nm (rod function) light-emitting diode (LED) flashes (2 degree diameter) were measured during a dark adaptation period after a 1-minute exposure to a bleaching light (3000 cd/m^2). Initially, 8 minutes of interleaved 625-nm and 527-nm thresholds were measured. After an additional 5 minutes of dark-adaptation, a second set of threshold measurements to 527-nm stimuli was performed during the subsequent 6 minutes.

Results. Dark-adapted b-wave amplitude was significantly reduced to all strengths of flash and a-wave in response to the strong flash stimulus was delayed (15.6 vs. 14.7 ms, $P < 0.05$) in patients with Down 30 compared with controls. Dark-adapted cone thresholds did not differ among the groups (−2.0, −1.8, and −1.7 log cd/m^2 for Down 30, Up 30, and controls, respectively, $P = 0.21$). In contrast, dark-adapted rod thresholds were elevated ($F_{(2,36)} = 8.537$, $P = 0.001$) in patients with Down 30 (mean = −3.2 ± 1.1 log cd/m^2) relative to controls (mean = −4.2 ± 0.3 log cd/m^2). Dark-adapted b-wave amplitudes were correlated with dark-adapted rod sensitivity in patients with DMD (Spearman Rho = 0.943, $P = 0.005$). The changes were much smaller or absent in patients with intact Dp260.

Conclusions. Dp260 is particularly required for normal rod-system function in dark adaptation.

Keywords: retina, rod, cone, electroretinogram (ERG), dark-adaptation, human vision, Duchenne muscular dystrophy (DMD), dystrophin protein

Duchenne muscular dystrophy (DMD) is a monogenic X-linked genetic condition caused by mutations of the *DMD* gene (MIM: 300377) affecting dystrophin protein (Dp) expression.[1,2] In addition to the characteristic progressive muscular dysfunction,[3] patients with DMD show nonprogressive cognitive disturbances[4] and altered retinal physiology[5,6] because dystrophins play an important role in synaptic structures[7–13] and in glial cell membranes[14,15] in the mammalian central nervous system (CNS), including the retina.

Reduced or nearly abolished scotopic full-field flash electroretinogram (ERG) b-wave, the positive ERG component, is a classic feature of DMD that has been confirmed by several groups in the past decades in patients[5,6,16–26] and in mouse models of DMD.[8,27–30]

The negative dark-adapted ERG in which the b-wave is smaller than the electro-negative a-wave, found in patients with DMD and mouse models of DMD, has been mainly associated with the alteration of Dp427,[24,27] a dystrophin protein encoded by a promoter located at the beginning

(exon 1) of the *DMD* gene, and Dp260,[8,23,24,29,31] expressed by an independent internal promoter located at exon 30 of the *DMD* gene.[32] Both Dp427 and Dp260 are primarily expressed in the outer plexiform layer of the mammalian retina[6–8] and possibly in the inner nuclear layer.[13]

A shorter *DMD* gene product, the Dp140 (promoter at exon 45), that is strongly expressed in the developing brain of the mouse and associated with cognitive dysfunctions in patients with DMD,[33,34] is also expressed in the retina.[13] However, its specific role in retinal physiology has not been elucidated. In addition, a short *DMD* gene product, Dp71, is strongly expressed in Muller glial cells of the mammalian retina.[7] Its promoter is located far downstream in the gene (between exons 62 and 63). Because distal mutations are rare in humans, the specific roles of this dystrophin protein in the human visual system have not been investigated in detail. There is evidence that genetic alterations presumably preventing expression of Dp71 result in a severe ERG phenotype[24] and its selective absence resulted in altered ERGs in Dp71-null mice.[35]

Despite structural[12,13,36] and functional[18,30,37] evidence that abnormal synaptic transmission between photoreceptors and bipolar cells is associated with *DMD* gene mutations, obvious clinically relevant visual dysfunctions, such as altered visual acuity, are not found in patients with DMD. However, red-green color deficiency[38] and reduced spatial luminance contrast sensitivity[37,39] have been reported by our group. Relatively preserved vision associated with impaired on-mediated photopic ERGs in patients with DMD[18,37] may be due to structural and functional differences between central and peripheral (or extra-foveal) retinal organization (i.e. photoreceptor to bipolar cell ratios in the primate retina[40]).

About 25 years ago, 2 studies showed normal dynamic dark-adaptation processes in patients with DMD.[21,41] In the first study,[41] normal thresholds to, presumably, white flashes were measured during 40 minutes of dark-adaptation after 5 minutes of bleach (600 cd/m^2) in 3 patients with a clinical diagnosis of DMD (two of them with abnormal ERGs) but without genetic confirmation. The second study[21] showed normal averaged thresholds during dark adaptation in DMD and patients with Becker muscular dystrophy (BMD; a mild variant of the disease) among other preserved visual functions. Unfortunately, details on their dark-adaptation procedure were not reported. It is unclear if the measured thresholds in these studies were mediated by cone or by rod activity. The severe dysfunction of rod-driven ERGs suggests that psychophysical dark-adaption thresholds may be changed when mainly mediated by rod activity. Furthermore, the individual thresholds may then be correlated with ERG parameters. Finally, the functional deficits may depend on which dystrophins are affected and thus on the location of the gene mutation.

In the present study, we measured full-field ERGs and psychophysical dark-adapted visual thresholds (separately for cone and rod pathways) in genetically characterized patients with alterations of the DMD gene either upstream of exon 30, thereby exclusively affecting the expression of Dp427 (DMD Up 30), or downstream of exon 30 (DMD Down 30), affecting the expression of Dp427 and Dp260 and possibly of Dp140 and Dp116. The results have been partially published as an ARVO abstract (IOVS 61: 5047 e-abstract).

Methods

Subjects

The experiments were performed in accordance with the tenets of the Declaration of Helsinki and were approved by the Human Research Ethics Committee of the Institute of Psychology at the University of São Paulo (CAEE no. 85512617.6.0000.5561), Brazil. All subjects, or their legal guardians, gave written informed consent prior to the examinations.

A group of 21 patients with DMD (mean age = 13.8 ± 4.3 years, all male patients) and 27 age matched ($F_{(2,47)}$ = 0.999, P = 0.376) healthy volunteers (mean age = 16.1 ± 5.5 years, 13 male patients) participated in this study. We have pooled the data from male and female control subjects because similar ERG responses and dark-adapted visual thresholds were obtained in the two groups (see Supplementary Material).

The subjects underwent a full ophthalmological examination, including of refraction, measurements of best-corrected visual acuity, and measurements of intraocular pressure, slit-lamp biomicroscopy, and funduscopic examination. ERGs and dark-adapted psychophysical thresholds were measured monocularly as an attempt to shorten the time of preparation and examination to avoid fatigue. The dominant eye was selected to obtain the best possible performance. Inclusion criteria were normal best-corrected distant visual acuity of 20/20 or better; absence of ocular hypertension and of ocular diseases, such as cataract, in the tested eye; absence of diseases that could affect the CNS (other than DMD for the experimental group); and no medications targeting the CNS.

The Table shows demographic information of two DMD groups that were determined according to the location of the genetic alteration in the *DMD* gene. Determination of the affected dystrophin proteins was based on the genomic organization of the human *DMD* gene (Fig. 1, based on Muntoni et al., 2003). Seven patients with DMD (DMD Up 30; mean age = 13.9 ± 6.3 years) displayed genetic alterations upstream of exon 30 with, presumably, only Dp427 affected. The other 14 patients with DMD (DMD Down 30; mean age = 13.7 ± 3.1 years) displayed genetic alterations downstream of exon 30 indicating that additional dystrophin proteins were affected (as indicated in the Table and Fig. 1). Patients who underwent both ERG and dark-adapted examinations (N = 10), are indicated by a symbol that corresponds to the symbols used in correlation plots (see Fig. 6). The other patients either participated in the ERG recordings or in the psychophysical measurements.

ERG Recordings

Dark-adapted and light-adapted flash ERGs according to International Society of Clinical Electrophysiology of Vision (ISCEV) standards (McCulloch et al., 2015) were recorded monocularly from the dilated dominant eyes of 28 subjects (15 patients with DMD and 13 controls). Control ERGs were recorded from six male and seven female (N = 13 control subjects) healthy volunteers. The remaining 14 control subjects undergoing only the psychophysical examination were tested before ERG protocols were included in the study.

Investigative Ophthalmology & Visual Science

Table. General Characteristics of Both DMD Groups: DMD Up 30 and DMD Down 30

	N	Age (y)	Mutation	Affected dystrophin proteins	Examination	Symbol code
DMD Up 30	1	22	3-7	Dp427	Both	○
	2	19	3-7	Dp427	Psychophysical	
	3	19	6	Dp427	Both	□
	4	8	6	Dp427	Psychophysical	
	5	8	7	Dp427	Both	△
	6	7	16	Dp427	Psychophysical	
	7	14	20	Dp427	Both	◇
DMD Down 30	8	14	12-39	Dp427 + Dp260	Both	○
	9	18	39	Dp427 + Dp260	Electrophysiological	
	10	12	40	Dp427 + Dp260	Both	□
	11	17	17-50	Dp427 + Dp260 + Dp140	Electrophysiological	
	12	11	34-44	Dp427 + Dp260 + Dp140	Electrophysiological	
	13	14	45-46	Dp427 + Dp260 + Dp140	Both	△
	14	9	45-52	Dp427 + Dp260 + Dp140	Both	◇
	15	13	45-52	Dp427 + Dp260 + Dp140	Psychophysical	
	16	19	47-50	Dp427 + Dp260 + Dp140	Both	⬠
	17	13	48-50	Dp427 + Dp260 + Dp140	Electrophysiological	
	18	16	48-52	Dp427 + Dp260 + Dp140	Psychophysical	
	19	10	49-50	Dp427 + Dp260 + Dp140	Psychophysical	
	20	16	52	Dp427 + Dp260 + Dp140	Both	⬡
	21	10	57	Dp427 + Dp260 + Dp140 + Dp116	Electrophysiological	

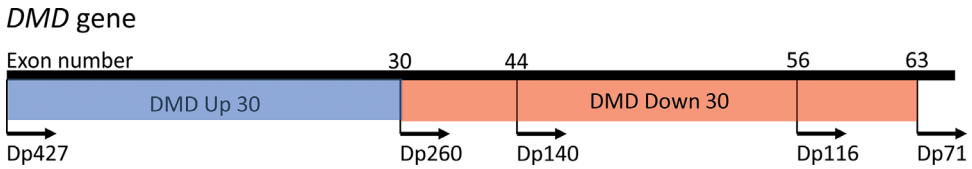

Figure 1. Genomic organization of the *DMD* gene.[32] Numbers indicate the exons after which internal promoters are located and *arrows* indicate the dystrophin protein (Dp) encoded by the gene fragment activated by the respective promoter. The *blue* area shows the localization of the genetic alterations (upstream exon 30) in 7 patients with DMD Up 30 and the *red* area shows the localization of genetic alterations (downstream exon 30) of 14 patients with DMD Down 30. Observe that the mutations in the DMD Down 30 of our patients were always located upstream of exon 63, meaning that all patients had presumably a normal expression of the shortest *DMD* gene product (Dp71).

First, the subjects were dark-adapted for 20 minutes. Flash stimuli of 0.01 cd.s/m^2, 3.0 cd.s/m^2, and 10 cd.s/m^2 were presented in sequence with an inter-stimulus time of 2, 10, and 20 seconds, respectively. Subsequently, the subjects underwent light-adaptation to a background of 30 cd/m^2 for 10 minutes. Then ERG responses to 3.0 cd.s/m^2 flashes (standard flash) were recorded with inter-stimulus time of 0.5 seconds. ERG responses were recorded with Dawson-Trick-Litzlkow (DTL) fiber electrodes placed under the lower lid and attached to the outer and the inner canthus. The reference and the ground (gold cup) skin electrodes were attached to the ipsilateral temple and forehead, respectively. Signals were amplified 100,000 times, filtered between 1 and 300 Hz, and sampled at 512 Hz using the RetiPort system (Roland Consult, Brandenburg, Germany). ERG responses were averages of five 256-ms epochs for the 10 cd.s/m^2 flashes and of 10 such epochs for the weaker flashes.

Detection Thresholds During Dark Adaptation

Flash detection thresholds during dark adaptation after a bleach were monocularly measured in nondilated dominant eyes of 38 subjects (16 patients with DMD and 22 controls). From 21 patients with DMD included in the study, 5 patients were not able to perform the psychophysical examination because of cognitive and / or motoric limitations. The equipment was the Roland dark adaptometer (Roland Consult, Brandenburg, Germany) equipped with a Q450 Ganzfeld stimulator. A fixation camera for pupil detection monitored fixation during the session. The subjects were instructed to press a key when they saw a flash. Thresholds to 625 nm peak wavelength (for cone-mediated detection) and 527 nm peak wavelength (for rod-dominant detection) light-emitting diode (LED) flashes (2 degrees diameter) were measured. Stimuli were presented at an eccentricity of 20 degrees in the temporal retina. The thresholds were measured during dark adaptation after 1 minute of bleach to 3000 cd/m^2 white light. We have adapted the bleach period (originally 5 minutes) and bleach luminance (originally 7000 cd/m^2) so that it was tolerated by the young subjects. In a pilot study, four different luminances (700, 3000, 5000, and 7000 cd/m^2) of the bleach light were used, keeping 1 minute of bleach time, to examine the control subjects ($N = 5$). We found that dark-adapted cone ($P = 0.779$) and rod ($P = 0.960$)

Investigative Ophthalmology & Visual Science

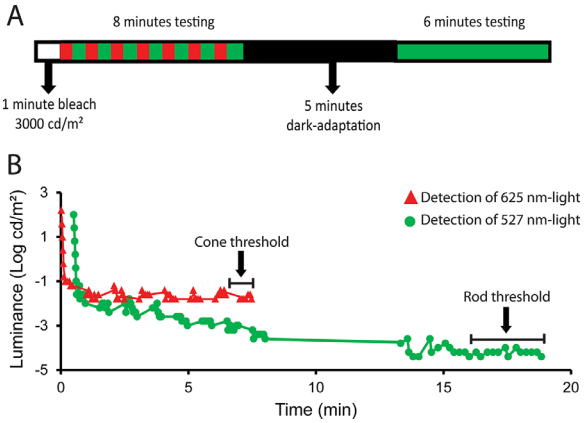

Figure 2. Dark-adapted visual thresholds. Thresholds were determined in darkness after 1 minute of bleach to 3000 cd/m^2 full field. The dark-adaptation curve was measured by the presentation of 250 ms flashes of 625-nm and 527-nm lights alternating every 30 seconds. After 8 minutes of measurements and 5 minutes interval in darkness, thresholds were measured by the presentation of 250 ms flashes of only 527 nm flashes (**A**). Representative thresholds measured with a control subject (**B**). *Red triangles* show the 625-nm light detection thresholds while *green circles* thresholds to the 527 nm flashes. Dark-adapted cone threshold was the averaged threshold luminances during the last minute of the first protocol. Dark-adapted rod threshold was the averaged luminances for measurements during the last 3 minutes of the second protocol.

thresholds as well as rod recovery time to −3 log cd/m^2 ($P = 0.542$) were similar with 3000 cd/m^2 and 7000 cd/m^2 bleach in control subjects (Supplementary Material).

After 1 minute of bleach, the tests started with 8 minutes of interleaved 625 nm and 527 nm stimuli presentations to measure cone-mediated and rod-dominant thresholds in parallel (Fig. 2B, red triangles and green circles, respectively). Within this period, a full recovery of cone-mediated thresholds was obtained. Because 527 nm light flash stimulates both rods and cones it produces a double function, whereas we see a single function with 627 nm, which does not stimulate the rods significantly. We are therefore calling cone function the curve that precedes the break, regardless of wavelength, and rod function the curve that follows the break, which results from stimulation that is not sufficiently intense to activate the cones. After an additional 5 minutes of dark adaptation, a second set of measurements was performed with only 527 nm stimuli for 6 minutes to measure rod-mediated thresholds. The thresholds generally reached a plateau within this period.

The procedure started with the determination of a threshold to 625 nm flashes. After 30 seconds, the procedure was repeated for 527 nm flashes. The alternation in threshold measurements in 30-second periods was continued throughout the first part of the test. Flashes were presented once every 2 seconds (flash duration = 250 ms). After every flash, the subject was requested to indicate if the flash was detected by pressing a button within 750 ms. Absence of a response was interpreted that the flash was not detected. If a flash was detected, the flash strength was decreased by 6 dB. If the flash was not detected, the flash strength increased by 2 dB.

Dark-adapted cone threshold was calculated by averaging the intensities (in log cd/m^2, only when the flash was seen) required to detect (the change from not detected to detected luminance) the 625 nm flash during the last minute of the first period. Dark-adapted rod threshold was obtained by averaging detection intensities (log cd/m^2) during the last 3 minutes of the second protocol.

Statistical Analysis

ERG amplitudes and phases and visual thresholds are presented as means ± one standard deviation. Group comparisons were performed using 1-way ANOVAs. Paired comparisons were performed using Bonferroni post hoc analyses. Significant correlations among variables were evaluated with Spearman's Rho (SPSS, Statistical Package for the Social Sciences, Hong Kong, China). P values < 0.05 were considered significant.

Results

Electrophysiologically Measured Retinal Responses to Light

Dark-adapted ERG responses to the weak (0.01 cd.s/m^2) flash (Fig. 3A) elicited a positive (b-wave) component with the peak at about 90 ms after flash onset. Mean (± one standard deviation) amplitudes differed significantly between the groups ($F_{(2,26)} = 10.519$, $P = 0.001$). B-wave amplitudes of control subjects (mean = 235.8 ± 100.4 µV) were significantly higher ($P < 0.001$) than those of the patients with DMD Down 30 (mean = 52.2 ± 36.9 µV). Intermediate amplitudes were found in the DMD Up 30 group (mean = 195.8 ± 168.2 µV). Their mean amplitude did not significantly differ from those of control subjects ($P = 0.998$) and of patients with DMD Down 30 ($P = 0.053$). There was no significant group effect on b-wave implicit times ($F_{(2,26)} = 2.131$, $P = 0.141$).

Figure 3B shows averaged responses of control subjects and patients to the dark-adapted 3.0 cd.s/m^2 flash showing a-wave and b-wave peaking at about 18 and 40 ms, respectively. In control subjects, the mean b-wave amplitude was 351.3 ± 116.4 µV and the mean a-wave amplitude was 214.7 ± 69.6 µV. Individual b:a ratios varied between 1.3 and 2 for the control subjects. Amplitudes ($F_{(2,26)} = 2.485$, $P = 0.105$) and times ($F_{(2,26)} = 0.821$, $P = 0.452$) of the a-wave were comparable among the groups. All patients with DMD Down 30 showed a single-peak a-wave in the DA 3.0 cd.s/m^2, whereas all 4 patients with Up 30 and 7 out of 13 control subjects showed bifid a-wave. In contrast to the normal a-wave amplitudes, b-waves were remarkably different among the groups ($F_{(2,26)} = 14.947$, $P < 0.001$). B-wave amplitudes of patients with DMD Down 30 (mean = 144.7 ± 57.5 µV) were significantly decreased ($P < 0.001$). Similar to the results obtained with the weak flash, patients with DMD Up 30 showed intermediate b-wave amplitudes (mean = 223.5 ± 41.6 µV), not differing statistically from those of control subjects ($P = 0.064$) or of patients with DMD Down 30 ($P = 0.466$). The mean b-wave implicit times were similar among the three groups ($F_{(2,26)} = 3.004$, $P = 0.069$).

The b:a ratio data had an approximately normal distribution and according tests were applied. The mean b:a ratios (Fig. 3B) were significantly different between groups ($F_{(2,26)} = 36.183$, $P < 0.001$). The b:a ratio was < 1 for 9 out of 10 patients with DMD Down 30 (mean = 0.6 ± 0.3) and ≥ 1 for all patients with DMD Up 30 (mean = 1.3 ± 0.5) and all control subjects (mean = 1.7 ± 0.2). Mean b:a ratios were significantly lower for patients with DMD Down 30

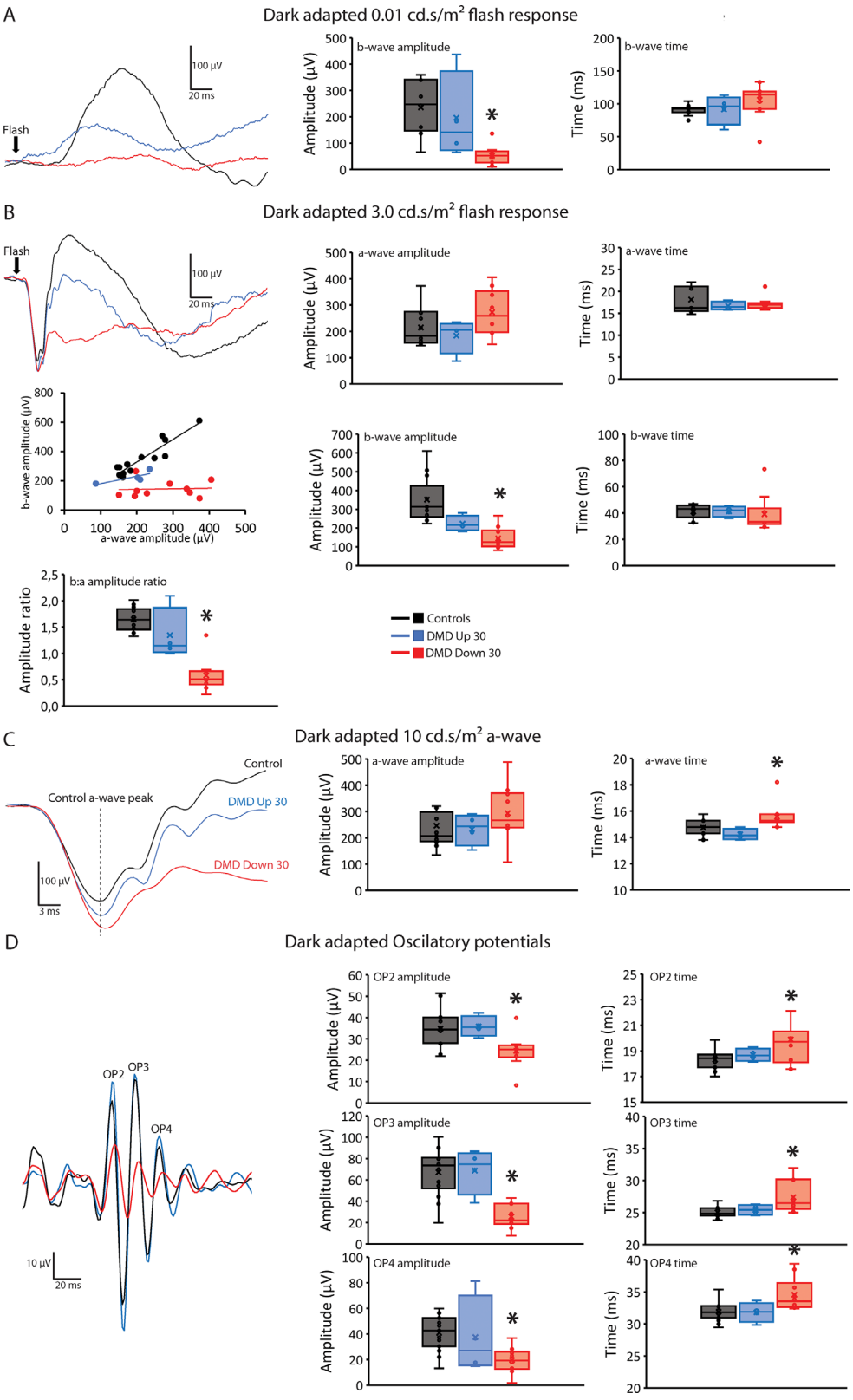

Figure 3. Dark-adapted ERG results. Averaged traces and mean/median (box = interquartile range [IQR]; whisker = minimum and maximum values) amplitudes, implicit times, and b:a ratios for controls (*black symbols*), patients with DMD Up 30 (*blue symbols*), and patients with DMD Down 30 (*red symbols*) for dark-adapted ERG measurements with 3 flash strengths: 0.01 cd.s/m^2 (b-wave only) (**A**), 3.0 cd.s/m^2 (**B**) 10 cd.s/m^2 (a-wave only) (**C**). and oscillatory potentials (**D**) extracted from responses to 3.0 cd.s/m^2 flash. Asterisk (*) indicates significant difference ($P < 0.05$) compared to the control group.

Investigative Ophthalmology & Visual Science

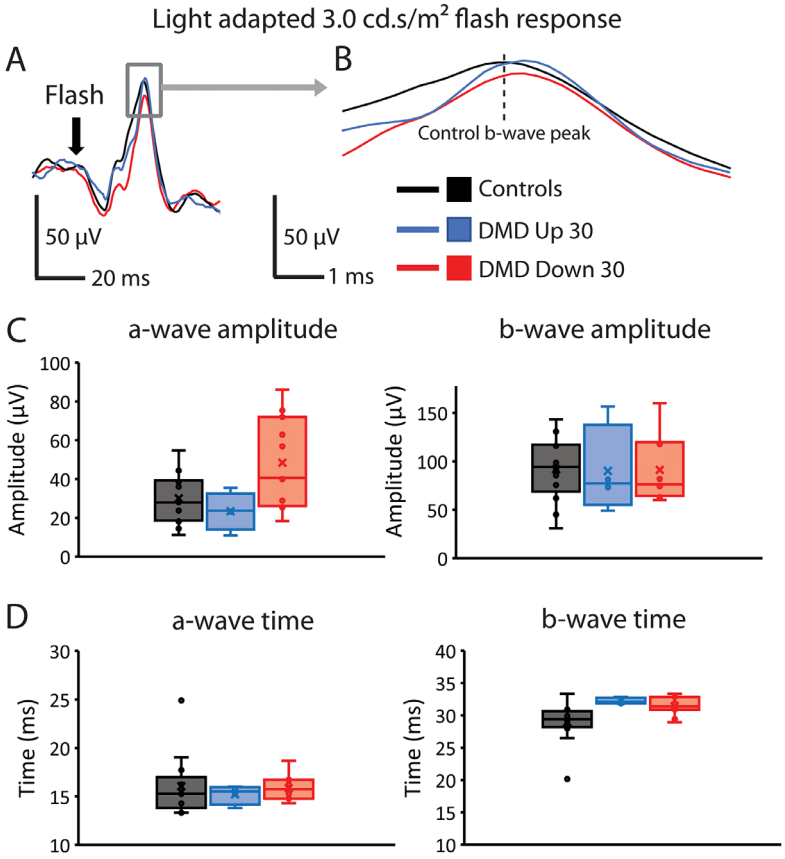

Figure 4. Light-adapted ERGs. Averaged traces (**A**: original responses; **B**: details of the b-wave) and mean / median (box = interquartile range [IQR]; whisker = minimum and maximum values) amplitudes (**C**) and implicit times (**D**) are shown for controls (*black symbols*), patients with DMD Up 30 (*blue symbols*), and patients with DMD Down 30 (*red symbols*) in the light-adapted protocol.

compared with both controls ($P < 0.001$) and patients with DMD Up 30 ($P = 0.001$).

Dark-adapted a-waves and b-waves elicited by a strong (10 cd.s/m^2) flash were recorded and the respective amplitudes and implicit times were compared between the groups. Figure 3C shows that there was a significant group effect ($F_{(2,26)} = 5.610$, $P = 0.010$) in the time to peak of the a-wave, whereas the amplitudes did not differ significantly between the groups ($F_{(2,26)} = 0.900$, $P = 0.420$). The mean a-wave implicit time measured in the control group was 14.7 ± 0.6 ms, similar ($P = 0.711$) to what has been observed for patients with DMD Up 30 (mean = 14.2 ± 0.4 ms). In contrast, patients with DMD Down 30 showed significantly longer a-wave peak times (mean = 15.6 ± 1.0 ms, $P = 0.019$) and with a marginal difference ($P = 0.050$) compared to patients with DMD Up 30. The dark-adapted b-wave elicited by the 10 cd.s/m^2 condition confirmed the results obtained with the standard 3.0 cd.s/m^2 flash: there was a group effect on b-wave amplitudes ($F_{(2,26)} = 6.766$, $P = 0.005$) with patients with DMD Down 30 showing significantly lower b-waves compared to controls ($P = 0.004$), but not compared to patients with DMD Up30 ($P = 0.863$). The last group showed intermediate b-wave amplitudes. The mean b-wave implicit time showed group effect ($F_{(2,26)} = 4.067$, $P = 0.030$), however, paired comparisons using Bonferroni post hoc analyses revealed that all three groups had statistically similar peak times ($P > 0.058$). In addition, b:a ratios calculated for DA 10 cd.s/m^2 strong flash amplitudes were significantly lower for patients with DMD Down 30 compared to both controls ($P < 0.001$) and patients with DMD Up 30 ($P = 0.019$).

Mean DA oscillatory potentials (OPs) from controls (black trace), patients with DMD Up 30 (blue trace), and patients with DMD Down 30 (red trace) extracted from DA 3.0 cd/m^2 are shown in Figure 3D. DA OPs were significantly reduced (group effect, $F_{(2,25)} = 16.168$ and $P < 0.001$) and delayed (group effect, amplitude $F_{(2,25)} = 6.426$ and $P = 0.005$) in patients with DMD Down 30 compared to controls (OP amplitudes $P < 0.001$ and implicit times $P = 0.005$) and compared to patients with DMD Up 30 for the amplitudes ($P = 0.003$), but not for the implicit times ($P = 0.119$).

Averaged light-adapted ERG responses are shown in Figure 4A with a more detailed representation of the b-wave in Figure 4B. The average waveforms were similar for the three groups. A significant group effect was observed for the a-wave amplitude ($F_{(2,26)} = 4.496$, $P = 0.021$). Patients with DMD Down 30 showed slightly larger a-wave amplitudes (Fig. 4C) with marginal statistical differences compared to control subjects ($P = 0.052$) and patients with DMD Up 30 ($P = 0.067$). In contrast, a-wave peak times were comparable ($F_{(2,26)} = 0.191$, $P = 0.827$) among the three groups (Fig. 4D). Light-adapted b-wave amplitudes (see Fig. 4C) were also comparable in the three groups ($F_{(2,26)} = 0.004$, $P = 0.996$). Patients with DMD Down 30 showed a nonsignificant ($P = 0.059$) delay of the b-wave compared to control subjects (Fig. 4D). Relatively delayed

Investigative Ophthalmology & Visual Science

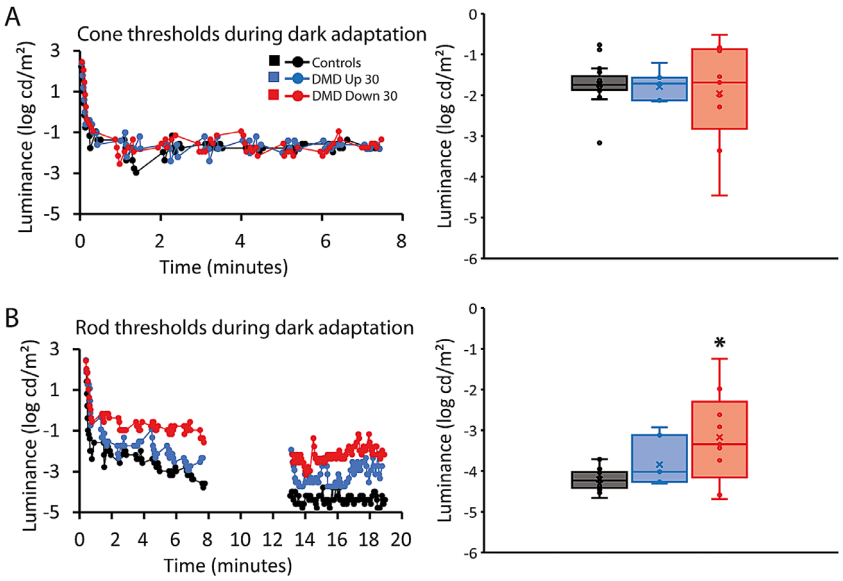

Figure 5. Course of detection thresholds during dark adaptation. Cone (**A**) and rod (**B**) thresholds as a function of time in the dark are shown for controls (*black traces*), patients with DMD Up 30 (*blue traces*), and patients with DMD Down 30 (*red traces*). The traces are thresholds from representative subjects from each group. The right plots show mean/median (box = interquartile range [IQR]; whisker = minimum and maximum values) during the last minute of the cone thresholds and of the last three minutes of the rod thresholds. Asterisk (*) indicates significant difference ($P < 0.05$) compared to the control group.

LA b-wave implicit times were more pronounced in the DMD Up 30 group. However, only 4 patients with DMD Up 30 were included in the analysis. Therefore, LA response impairments cannot be reliably evaluated.

Comparable light-adapted OP amplitudes ($P = 0.518$) and implicit times ($P = 0.181$) between patients with DMD Down 30 and controls have been found. For patients with DMD Up 30, we found significantly reduced light-adapted OPs compared to controls ($P = 0.036$), whereas there were no significant changes in implicit times ($P = 0.999$). However, because only 4 patients with DMD Up 30 were included in the study, a definitive conclusion regarding LA ERG alterations in patients with DMD Up 30 cannot be established.

Psychophysically Measured Dark Adaptation of Cone and Rod Thresholds

Figure 5 shows the course of cone (responses to 625-nm light; see Fig. 5A) and rod (responses to 527-nm light; see Fig. 5B) detection thresholds for one representative subject of each group. Observe that the cone thresholds are similar for all three subjects (see Fig. 5A). Accordingly, the dark-adapted cone thresholds, calculated by averaging stimulus luminances at the last minute of the first protocol, were statistically similar ($F_{(2,36)} = 0.388$, $P = 0.681$) among the three groups: control subjects (mean = −1.7 ± 0.5 log cd/m^2), patients with DMD Up 30 (mean = −1.8 ± 0.4 log cd/m^2), and patients with DMD Down 30 (mean = −2.0 ± 1.3 log cd/m^2). In addition, there was no group effect ($F_{(2,36)} = 1.634$, $P = 0.210$) when the same method was applied to calculate dark-adapted (initial) rod thresholds averaging stimulus luminances at the last minute of the first protocol. Although, patients with DMD both DMD Up 30 (mean = −2.5 ± 0.6 log cd/m^2) and DMD Down 30 (mean = −2.5 ± 1.4 log cd/m^2) showed slightly elevated thresholds compared to control subjects (mean = −3.0 ± 0.5 log cd/m^2).

We have previously demonstrated[42] that with the type of bleaching used in this study, rod-cone break can be observed at about 2.5 minutes after bleaching offset in healthy subjects. In Figure 5B, responses elicited by 527 nm stimulus represent a mixture of rod and cone function, with a small contribution from the cones. However, stimuli detected at a luminance level of about -4 log cd/m^2, as found in controls and patients with DMD Up 30, are probably too low for cone detection. Therefore, it may be considered a rod threshold. The dark-adapted rod thresholds, calculated by averaging stimulus luminances at the 3 last minutes of the second set of measurements, were significantly elevated (group effect: $F_{(2,36)} = 8.537$, $P = 0.001$) in patients with DMD Down 30 (mean = −3.2 ± 1.1 log cd/m^2, $P = 0.001$) compared to control subjects (mean = −4.2 ± 0.3 log cd/m^2), but not compared to patients with DMD Up 30 (mean = −3.8 ± 0.6 log cd/m^2, $P = 0.130$). Patients with DMD Up 30 thresholds were statistically similar ($P = 0.566$) to control thresholds as well.

Correlations

Properties of ERG components were correlated with visual sensitivity (Fig. 6). As shown in the Table, 6 patients with DMD Down 30 and 4 patients with DMD Up 30 participated in the ERG and the psychophysical measurements. Six control subjects underwent both measurements. There was a significant positive correlation between dark-adapted b-wave amplitudes to 0.01 cd.s/m^2 flashes and the dark-adapted rod sensitivity (1/threshold luminance in cd/m^2) for patients with DMD Down 30 (red symbols; Spearman's Rho = 0.943, $P = 0.005$). Similar tendency was observed for the patients with DMD Up 30 (blue symbols). For the control subjects we did not observe significant correlation (black symbols; Spearman's Rho = 0.290, $P = 0.577$). Other ERG

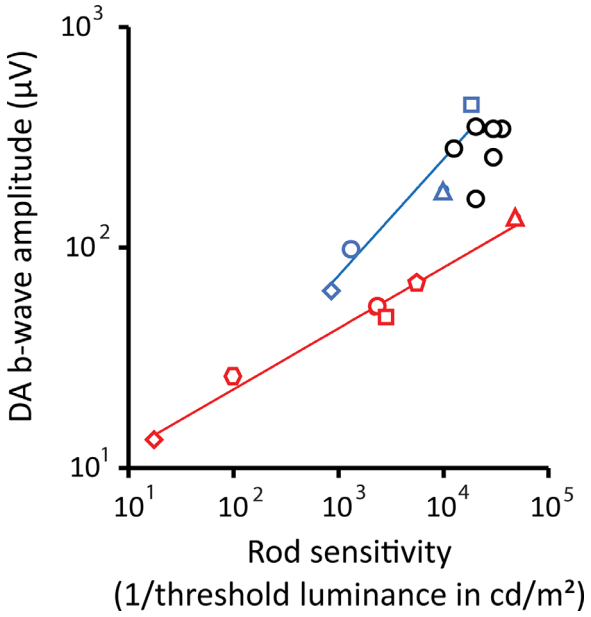

Figure 6. Correlations between dark-adapted ERG b-wave and rod sensitivity. Dark-adapted b-wave amplitudes of ERG responses to 0.01 cd.s/m^2 flashes plotted as a function of dark-adapted rod sensitivity (1/threshold luminance in cd/m^2) for patients with DMD Down 30 (*red symbols*, $N = 6$), patients with DMD Up 30 (*blue symbols*, $N = 4$), and control subjects (*black symbols*, $N = 6$). A positive correlation was found for the patients but not for the control subjects.

parameters were not correlated with dark-adapted cone or rod thresholds for any of the groups.

Discussion

In the present study, a significant reduction in the dark-adapted b-wave amplitude of patients with DMD Down 30 (lacking at least dystrophin protein Dp260 in addition to Dp427 alteration) was found when compared to control subjects. We also reported that psychophysical dark-adapted rod thresholds were significantly elevated in patients with DMD Down 30. A positive correlation between b-wave amplitude to 0.01 cd.s/m^2 flashes and rod sensitivity was found for the patients. These results offer new insights regarding cone and rod function in retinae of patients with DMD.

The dark-adapted ERG b-wave to 0.01 cd.s/m^2 flashes mainly reflects the integrity of the depolarizing on-bipolar cells of the rod system.[43] This ERG component was found to be severely reduced (~30% of the control amplitude, in average) in patients with DMD Down 30, emphasizing the role that Dp260 plays in the rod to rod-bipolar cell synapse. In addition, the reduced b-wave with preserved a-wave of the 3.0 cd.s/m^2 flash (electronegative) ERG, as found in several conditions affecting the synapses between photoreceptors and bipolar cells[44–55] confirms this notion. The correlation between ERG b-waves and psychophysical results does not mean that the two parameters are causally linked. However, they may be indirectly linked by sharing a cause, even if they are driven by two completely different mechanisms. The dysfunctional synapse of the rods to rod bipolar cells possibly underlies the alteration in the rod driven ERG and psychophysical pathways.

The dark-adapted ERG a-wave to standard flash depends on photoreceptor as well as post-receptoral integrity.[56–58] A strong flash (10 cd.s/m^2 and above) allows enhancing a-waves reflecting photoreceptor function,[59] because at this flash strength the a-wave reflect rod sensitivity, not depending so much on post-receptoral interactions.[57] Patients with DMD Down 30 showed delayed a-wave peak in response to the dark-adapted 10 cd.s/m^2 flash ERG, which may be due to a delay in the impaired b-wave in these patients. Thus, the photoreceptoral function is presumably unaffected. Reduced dark-adapted OPs in patients with DMD Down 30 may reflect inner retinal disturbances[60,61] or a consequence of the outer retinal (photoreceptor to bipolar cells) defects influencing inner retinal activation and, therefore, resulting in b-wave and OP alteration, respectively. Moreover, decreased OPs may have altered the bifid a-wave waveform in patients with DMD Down 30.

Primate light-adapted (photopic or cone) ERG reflects cone integrity and function of the post-receptoral (on-bipolar, off-bipolar, and horizontal cells) neurons.[62] Patients with DMD showed normal to slightly enhanced light-adapted ERG a-wave amplitudes with normal implicit times, as previously described.[17,24–26] Slightly delayed light-adapted ERG b-waves were found in patients with DMD as it has been previously reported.[17] It may reflect the unbalanced post-receptoral on-bipolar and off-bipolar cells' function in photopic conditions,[63] as previously reported in patients with DMD,[18,37] possibly due to the slow activation of the on-bipolar cells.[64] We hypothesize that relatively preserved photopic ERG responses in patients with DMD are due to the retinal mechanism (Off or hyperpolarizing bipolar cells) of the cone system compensating on-dysfunction and, therefore, resulting in close to normal light-adapted ERG responses.

The present data showed that *DMD* gene alterations presumably affecting the expression of the retinal dystrophin protein Dp260 (patients with DMD Down 30) is associated with preserved dark-adapted cone thresholds and elevated dark-adapted rod thresholds without symptoms of nyctalopia or bradyopsia. As reported by Bijveld et al., patients with the incomplete type of congenital stationary night blindness (iCSNB or CSNB2) display minimal or no symptoms of night vision disturbances despite their rod thresholds being elevated. The authors argued that visual symptoms may not be perceived by the patients because vision is disturbed only in very dark circumstances that are usually not experienced in modern daily routine.[65] It may also explain why patients with DMD do not complain about their night vision.[25]

Interestingly, unaffected dark-adapted visual sensitivity recovery after photobleaching has been reported in patients with DMD with altered ERGs.[21,41] In the first study showing dark-adapted thresholds in patients with DMD,[41] a few subjects were tested and only three patients displayed the characteristic negative ERG. In the second study,[21] eight boys with genetic alteration downstream exon 44 presumably affecting Dp427 and Dp260 showed normal dark-adaptation, but patients with BMD, displaying milder phenotype than patients with DMD due to the ability of the *DMD* gene to produce some functional dystrophin protein, were included in the study.

The discrepancy between our results and previously reported results[21,41] may be partially because of methodological differences to record dark-adapted thresholds. We measured dark-adapted cone (625 nm light) and rod (527 nm

Investigative Ophthalmology & Visual Science

light) thresholds separately, whereas the dark-adaptation thresholds to presumably white light has been previously measured. Alternatively or in addition, only patients with genetically characterized DMD have been examined in the present study, whereas, previously, either patients with DMD without genetic information[41] or pooled patients with DMD and patients with BMD[21] were studied.

We recognize that our protocol to measure dark-adapted cone and rod thresholds is a short (adapted) version of the original (~40 minutes) protocol that we have developed as an attempt to make the examination tolerable by the young patients and controls studied here.[42] Moreover, a larger population could be evaluated to provide more reliable statistical analysis. Future investigations could consider evaluating a large group of patients with DMD measuring final rod thresholds after long dark-adapted intervals, as in our protocols it was limited to approximately 20 minutes of dark adaptation, the same adaptation time used to measure the ERG b-wave to weak flash. However, we believe that a longer protocol would not change the sensitivity level arrived at 20 minutes of dark adaptation, at least with the bleaching strength we used. We found the thresholds to be stable at the end of the second protocol (mean slope of linear regression at the last 4 minutes of the second series: controls $= -0.0002 \pm 0.0006$; DMD Up 30 $= -0.0004 \pm 0.0023$; and DMD Down 30 $= 0.003 \pm 0.002$).

Regarding DMD causing asymmetric cone versus rod system dysfunction, we hypothesize that either compensatory functional mechanisms of the retina, perhaps provided by off-bipolar cells spared in patients with DMD,[18,37] or alternative retinal mechanisms for regenerating cone visual pigments[66] would guarantee relatively preserved light-adapted ERGs and normal dark-adapted cone thresholds.

Conclusions

Although the knowledge about affected versus preserved neural processes in the DMD retina contributes substantially to understand the pathophysiology of this retinal disease, ERG changes are not necessarily associated with detectable visual losses. For instance, severe dark-adapted and slight light-adapted ERG alterations caused by *DMD* gene mutations are not related to any obvious visual symptom. However, red-green color vision impairment[38] and contrast sensitivity losses[37,39] revealed that the cone pathway is affected in patients with DMD. In addition, we have now reported that rod sensitivity is also affected and, moreover, it correlates with the severe dark-adapted (scotopic or rod driven) ERG deficits, which is the classic nonmuscular sign of DMD. Dark-adapted rod threshold could be used to evaluate the efficacy of future treatments to rescue the expression of dystrophin proteins in the CNS.

Acknowledgments

The authors thank to Mayana Zatz and Rita Pavanello from the "Centro de Pesquisa sobre o Genoma Humano e Células-tronco" (University of Sao Paulo, Sao Paulo, Brazil) for the genetic tests and all the patients and their families who kindly consented to participate in this study.

Supported by Sao Paulo Research Foundation (FAPESP Grant Numbers 2016/04538-3 and 2014/26818-2 to DFV; 2017/16948-4 to LAS; 2015/22227-2 to KSV), National Council for Scientific and Technological Development (CNPq Grant Number 404239/2016-1 to MTSB), National Research, Development, and Innovation Fund of Hungary (OTKA PD13479 to MTSB), Tempus Public Foundation (Grant Number 465858 to MTSB), and NRDI Fund (TKP2020 IES, Grant No. BME-IE-BIO and TKP2020 NC, Grant No. BME-NC) based on the charter of bolster issued by the NRDI Office under the auspices of the Ministry for Innovation and Technology (Hungary) to BVN.

Disclosure: **M.T.S. Barboni**, None; **S.L. Dias**, None; **L.A. Silva**, None; **F.M. Damico**, None; **K.S. Vidal**, None; **M.F. Costa**, None; **B.V. Nagy**, None; **J. Kremers**, None; **D.F. Ventura**, None

References

1. Hoffman EP, Brown RH, Kunkel LM. Dystrophin: the protein product of the Duchenne muscular dystrophy locus. *Cell*. 1987;51:919–928.
2. Koenig M, Hoffman EP, Bertelson CJ, Monaco AP, Feener C, Kunkel LM. Complete cloning of the Duchenne muscular dystrophy (DMD) cDNA and preliminary genomic organization of the DMD gene in normal and affected individuals. *Cell*. 1987;50:509–517.
3. Chelly J, Gilgenkrantz H, Lambert M, et al. Effect of dystrophin gene deletions on mRNA levels and processing in Duchenne and Becker muscular dystrophies. *Cell*. 1990;63:1239–1248.
4. Lidov HG, Byers TJ, Watkins SC, Kunkel LM. Localization of dystrophin to postsynaptic regions of central nervous system cortical neurons. *Nature*. 1990;348:725–728.
5. Cibis GW, Fitzgerald KM, Harris DJ, Rothberg PG, Rupani M. The effects of dystrophin gene mutations on the ERG in mice and humans. *Invest Ophthalmol Vis Sci*. 1993;34:3646–3652.
6. Pillers DA, Bulman DE, Weleber RG, et al. Dystrophin expression in the human retina is required for normal function as defined by electroretinography. *Nat Genet*. 1993;4:82–86.
7. Claudepierre T, Rodius F, Frasson M, et al. Differential distribution of dystrophins in rat retina. *Invest Ophthalmol Vis Sci*. 1999;40:1520–1529.
8. D'Souza VN, Nguyen TM, Morris GE, Karges W, Pillers DA, Ray PN. A novel dystrophin isoform is required for normal retinal electrophysiology. *Hum Mol Genet*. 1995;4:837–842.
9. Kameya S, Araki E, Katsuki M, et al. Dp260 disrupted mice revealed prolonged implicit time of the b-wave in ERG and loss of accumulation of beta-dystroglycan in the outer plexiform layer of the retina. *Hum Mol Genet*. 1997;6:2195–2203.
10. Miike T, Miyatake M, Zhao J, Yoshioka K, Uchino M. Immunohistochemical dystrophin reaction in synaptic regions. *Brain Dev*. 1989;11:344–346.
11. Miyatake M, Miike T, Zhao JE, Yoshioka K, Uchino M, Usuku G. Dystrophin: localization and presumed function. *Muscle Nerve*. 1991;14:113–119.
12. Schmitz F, Drenckhahn D. Dystrophin in the retina. *Prog Neurobiol*. 1997;53:547–560.
13. Wersinger E, Bordais A, Schwab Y, et al. Reevaluation of dystrophin localization in the mouse retina. *Invest Ophthalmol Vis Sci*. 2011;52:7901–7908.
14. Ahn AH, Kunkel LM. The structural and functional diversity of dystrophin. *Nat Genet*. 1993;3:283–291.
15. Austin RC, Howard PL, D'Souza VN, Klamut HJ, Ray PN. Cloning and characterization of alternatively spliced isoforms of Dp71. *Hum Mol Genet*. 1995;4:1475–1483.
16. Cibis GW, Fitzgerald KM. The negative ERG is not synonymous with nightblindness. *Trans Am Ophthalmol Soc*. 2001;99:171–175; discussion 175-176.
17. De Becker I, Riddell DC, Dooley JM, Tremblay F. Correlation between electroretinogram findings and molecular analysis

in the Duchenne muscular dystrophy phenotype. *Br J Ophthalmol*. 1994;78:719–722.
18. Fitzgerald KM, Cibis GW, Giambrone SA, Harris DJ. Retinal signal transmission in Duchenne muscular dystrophy: evidence for dysfunction in the photoreceptor/depolarizing bipolar cell pathway. *J Clin Invest*. 1994;93:2425–2430.
19. Girlanda P, Quartarone A, Buceti R, et al. Extra-muscle involvement in dystrophinopathies: an electroretinography and evoked potential study. *J Neurol Sci*. 1997;146:127–132.
20. Ino-ue M, Honda S, Nishio H, Matsuo M, Nakamura H, Yamamoto M. Genotype and electroretinal heterogeneity in Duchenne muscular dystrophy. *Exp Eye Res*. 1997;65:861–864.
21. Jensen H, Warburg M, Sjö O, Schwartz M. Duchenne muscular dystrophy: negative electroretinograms and normal dark adaptation. Reappraisal of assignment of X linked incomplete congenital stationary night blindness. *J Med Genet*. 1995;32:348–351.
22. Pascual Pascual SI, Molano J, Pascual-Castroviejo I. Electroretinogram in Duchenne/Becker muscular dystrophy. *Pediatr Neurol*. 1998;18:315–320.
23. Pillers DA, Fitzgerald KM, Duncan NM, et al. Duchenne/Becker muscular dystrophy: correlation of phenotype by electroretinography with sites of dystrophin mutations. *Hum Genet*. 1999;105:2–9.
24. Ricotti V, Jägle H, Theodorou M, Moore AT, Muntoni F, Thompson DA. Ocular and neurodevelopmental features of Duchenne muscular dystrophy: a signature of dystrophin function in the central nervous system. *Eur J Hum Genet EJHG*. 2016;24:562–568.
25. Sigesmund DA, Weleber RG, Pillers DA, et al. Characterization of the ocular phenotype of Duchenne and Becker muscular dystrophy. *Ophthalmology*. 1994;101:856–865.
26. Tremblay F, De Becker I, Dooley JM, Riddell DC. Duchenne muscular dystrophy: negative scotopic bright-flash electroretinogram but not congenital stationary night blindness. *Can J Ophthalmol J Can Ophtalmol*. 1994;29:274–279.
27. Bucher F, Friedlander MS, Aguilar E, et al. The long dystrophin gene product Dp427 modulates retinal function and vascular morphology in response to age and retinal ischemia [published online ahead of print June, 11, 2019]. *Neurochem Int*, https://doi.org/10.1016/j.neuint.2019.104489.
28. Pillers DA, Weleber RG, Woodward WR, Green DG, Chapman VM, Ray PN. mdxCv3 mouse is a model for electroretinography of Duchenne/Becker muscular dystrophy. *Invest Ophthalmol Vis Sci*. 1995;36:462–466.
29. Pillers DA, Weleber RG, Green DG, et al. Effects of dystrophin isoforms on signal transduction through neural retina: genotype-phenotype analysis of Duchenne muscular dystrophy mouse mutants. *Mol Genet Metab*. 1999;66:100–110.
30. Tsai TI, Barboni MTS, Nagy BV, et al. Asymmetrical functional deficits of on and off retinal processing in the mdx3Cv mouse model of Duchenne muscular dystrophy. *Invest Ophthalmol Vis Sci*. 2016;57:5788–5798.
31. Barboni MTS, Liber AMP, Joachimsthaler A, et al. Altered visual processing in the mdx52 mouse model of Duchenne muscular dystrophy. *Neurobiol Dis*. 2021;105288.
32. Muntoni F, Torelli S, Ferlini A. Dystrophin and mutations: one gene, several proteins, multiple phenotypes. *Lancet Neurol*. 2003;2:731–740.
33. Doorenweerd N. Combining genetics, neuropsychology and neuroimaging to improve understanding of brain involvement in Duchenne muscular dystrophy - a narrative review. *Neuromuscul Disord NMD*. 2020;30:437–442.
34. Ricotti V, Mandy WPL, Scoto M, et al. Neurodevelopmental, emotional, and behavioural problems in Duchenne muscular dystrophy in relation to underlying dystrophin gene mutations. *Dev Med Child Neurol*. 2016;58:77–84.
35. Barboni MTS, Vaillend C, Joachimsthaler A, et al. Rescue of defective electroretinographic responses in Dp71-null mice with AAV-mediated reexpression of Dp71. *Invest Ophthalmol Vis Sci*. 2020;61:11.
36. Schmitz F, Drenckhahn D. Localization of dystrophin and beta-dystroglycan in bovine retinal photoreceptor processes extending into the postsynaptic dendritic complex. *Histochem Cell Biol*. 1997;108:249–255.
37. Barboni MTS, Nagy BV, de Araújo Moura AL, et al. ON and OFF electroretinography and contrast sensitivity in Duchenne muscular dystrophy. *Invest Ophthalmol Vis Sci*. 2013;54:3195–3204.
38. Costa MF, Oliveira AGF, Feitosa-Santana C, Zatz M, Ventura DF. Red-green color vision impairment in Duchenne muscular dystrophy. *Am J Hum Genet*. 2007;80:1064–1075.
39. Costa MF, Barboni MTS, Ventura DF. Psychophysical measurements of luminance and chromatic spatial and temporal contrast sensitivity in Duchenne muscular dystrophy. *Psychol. Neurosci*. 2011;4:67–74.
40. Telkes I, Lee SCS, Jusuf PR, Grünert U. The midget-parvocellular pathway of marmoset retina: a quantitative light microscopic study. *J Comp Neurol*. 2008;510:539–549.
41. Tremblay F, De Becker I, Riddell DC, Dooley JM. Duchenne muscular dystrophy: negative scotopic bright-flash electroretinogram and normal dark adaptation. *Can J Ophthalmol*. 1994;29:280–283.
42. Nagy BV, Ashman Z, Barboni MTS, Padua L, Vidal KSM, Ventura DF. Dark adaptation in Duchenne muscular dystrophy with a short protocol. *Invest Ophthalmol Vis Sci*. 2017;58:5408–5408.
43. Frishman LJ. Origins of the electroretinogram. In *Principles and practice of clinical electrophysiology of vision*. Cambridge, UK: MIT Press: 2006; pp. 139–183.
44. Alexander KR, Fishman GA, Barnes CS, Grover S. On-response deficit in the electroretinogram of the cone system in X-linked retinoschisis. *Invest Ophthalmol Vis Sci*. 2001;42:453–459.
45. Barnes CS, Alexander KR, Fishman GA. A distinctive form of congenital stationary night blindness with cone ON-pathway dysfunction. *Ophthalmology*. 2002;109:575–583.
46. Carr RE. Congenital stationary nightblindness. *Trans Am Ophthalmol Soc*. 1974;72:448–487.
47. Hotta K, Kondo M, Nakamura M, et al. Negative electroretinograms in pericentral pigmentary retinal degeneration. *Clin Experiment Ophthalmol*. 2006;34:89–92.
48. Lei B, Bush RA, Milam AH, Sieving PA. Human melanoma-associated retinopathy (MAR) antibodies alter the retinal ON-response of the monkey ERG in vivo. *Invest Ophthalmol Vis Sci*. 2000;41:262–266.
49. Martemyanov KA, Sampath AP. The transduction cascade in retinal on-bipolar cells: signal processing and disease. *Annu Rev Vis Sci*. 2017;3:25–51.
50. Miyake Y, Yagasaki K, Horiguchi M, Kawase Y, Kanda T. Congenital stationary night blindness with negative electroretinogram. A new classification. *Arch Ophthalmol Chic Ill 1960*. 1986;104:1013–1020.
51. Pardue MT, McCall MA, LaVail MM, Gregg RG, Peachey NS. A naturally occurring mouse model of X-linked congenital stationary night blindness. *Invest Ophthalmol Vis Sci*. 1998;39:2443–2449.
52. Pardue MT, Peachey NS. Mouse b-wave mutants. *Doc Ophthalmol Adv Ophthalmol*. 2014;128:77–89.
53. Sergouniotis PI, Robson AG, Li Z, et al. A phenotypic study of congenital stationary night blindness (CSNB) associated with mutations in the GRM6 gene. *Acta Ophthalmol (Copenh)*. 2012;90:e192–e197.

Investigative Ophthalmology & Visual Science

54. Shinoda K, Ohde H, Mashima Y, et al. On- and off-responses of the photopic electroretinograms in X-linked juvenile retinoschisis. *Am J Ophthalmol*. 2001;131:489–494.
55. Vincent A, Robson AG, Neveu MM, et al. A phenotype-genotype correlation study of X-linked retinoschisis. *Ophthalmology*. 2013;120:1454–1464.
56. Hood DC, Birch DG. The A-wave of the human electroretinogram and rod receptor function. *Invest Ophthalmol Vis Sci*. 1990;31:2070–2081.
57. Robson JG, Frishman LJ. The rod-driven a-wave of the dark-adapted mammalian electroretinogram. *Prog Retin Eye Res*. 2014;0:1–22.
58. Rodieck RW. Components of the electroretinogram–a reappraisal. *Vision Res*. 1972;12:773–780.
59. McCulloch DL, Marmor MF, Brigell MG, et al. ISCEV Standard for full-field clinical electroretinography (2015 update). *Doc Ophthalmol Adv Ophthalmol*. 2015;130:1–12.
60. Algvere P. Clinical studies on the oscillatory potentials of the human electroretinogram with special reference to the scotopic b-wave. *Acta Ophthalmol (Copenh)*. 1968;46:993–1024.
61. Wachtmeister L, Dowling JE. The oscillatory potentials of the mudpuppy retina. *Invest Ophthalmol Vis Sci*. 1978;17:1176–1188.
62. Bush RA, Sieving PA. A proximal retinal component in the primate photopic ERG a-wave. *Invest Ophthalmol Vis Sci*. 1994;35:635–645.
63. Sieving PA, Murayama K, Naarendorp F. Push-pull model of the primate photopic electroretinogram: a role for hyperpolarizing neurons in shaping the b-wave. *Vis Neurosci*. 1994;11:519–532.
64. Roux M, Philipps A, Chapot C, Sahel J, Rendon A. Alterations in the mGluR6 signaling complex in the retina of mdx3Cv mice, a model of Duchenne muscular disease. *Invest Ophthalmol Vis Sci*. 2013;54:5084–5084.
65. Bijveld MMC, van Genderen MM, Hoeben FP, et al. Assessment of night vision problems in patients with congenital stationary night blindness. *PLoS One*. 2013;8:e62927.
66. Morshedian A, Kaylor JJ, Ng SY, et al. Light-driven regeneration of cone visual pigments through a mechanism involving RGR opsin in Müller glial cells. *Neuron*. 2019;102:1172–1183.e5.

Investigative Ophthalmology & Visual Science